Wiley Series in Pure and Applied Optics

Glenn Boreman, Series Editor

WAVELENGTH DIVISION MULTIPLEXING

A PRACTICAL ENGINEERING GUIDE

KLAUS GROBE

MICHAEL EISELT

WILEY

WAVELENGTH DIVISION MULTIPLEXING

WILEY SERIES IN PURE AND APPLIED OPTICS

Founded by Stanley S. Ballard, University of Florida

EDITOR: Glenn Boreman, University of North Carolina at Charlotte

A complete list of the titles in this series appears at the end of this volume.

WAVELENGTH DIVISION MULTIPLEXING

A Practical Engineering Guide

KLAUS GROBE
MICHAEL EISELT

WILEY

Published by John Wiley & Sons, Inc., Hoboken, New Jersey
Published simultaneously in Canada

***Library of Congress Cataloging-in-Publication Data*:**

Grobe, Klaus.
Wavelength division multiplexing : a practical engineering guide / Klaus Grobe, Michael Eiselt. – 1st edition.
pages cm. – (Wiley-OSA series on optical communication ; 1)
Includes index.
ISBN 978-0-470-62302-2 (hardback)
1. Wavelength division multiplexing. I. Eiselt, Michael. II. Title.
TK5103.592.W38G76 2013
621.382′16–dc23

2013017946

Printed in the United States of America

10 9 8 7 6 5 4 3 2 1

CONTENTS

ACKNOWLEDGMENTS

Klaus Grobe wants to thank Hans-Peter Kuchenbecker and Casimer DeCusatis for their support that, directly and indirectly, led to this book. Special thanks also go to his father, Helmut, and his daughter, Kira.

Michael Eiselt wants to thank his managers and mentors Tingye Li, Hans-Georg Weber, Robert W. Tkach, and Robert M. Jopson for their support and guidance throughout his career. He also thanks his wife Renate and his daughters Susanna and Elisabeth for giving him encouragement and strength in his life.

The authors also want to acknowledge the support of their colleagues from ADVA. An extra thank-you goes to Marcus Sauter for the photographies. Finally, we thank the people at John Wiley & Sons, Inc. who supported this book, in particular Kari.

1

INTRODUCTION TO WDM

1.1 WDM THEORY

Wavelength division multiplexing (WDM) refers to a multiplexing and transmission scheme in optical telecommunications fibers where different wavelengths, typically emitted by several lasers, are modulated independently (i.e., they carry independent information from the transmitters to the receivers). These wavelengths are then multiplexed in the transmitter by means of passive WDM filters, and likewise they are separated or demultiplexed in the receiver by means of the same filters or coherent detection that usually involves a tunable local oscillator (laser).

WDM is an efficient means for increasing the transport capacity, or usable bandwidth, particularly of optical single-mode fibers. It also allows the separation of different customers' traffic in the wavelength (or optical frequency) domain and as such can be used as a multiple-access mechanism. The respective scheme is called wavelength-division multiple access (WDMA).

Modulated and multiplexed signals must be separated from each other or demultiplexed in order to be demodulated (otherwise, cross talk may appear). For separation, each pair of the respective signals must support orthogonality. For any two signals to be orthogonal, their scalar product must be zero:

$$(\underline{f},\ \underline{g}^*) = \underline{f}^{\mathrm{T}} \cdot\ \underline{g}^* = \sum_i f_i \cdot g_i^* \overset{!}{=} 0, \quad \text{with} \quad f_i \cdot g_i^* = \int_a^b f_i(x) \cdot g_i^*(x)\mathrm{d}x,\ \ i = 1, \cdots, N. \tag{1.1}$$

Wavelength Division Multiplexing: A Practical Engineering Guide, First Edition.
Klaus Grobe and Michael Eiselt.

(f, g^*) is the scalar product of complex functions, where * denotes complex conjugation. Equation (1.1) is also written for vector functions in order to be able to consider effects of orthogonally polarized signals.

The vanishing scalar product of the two signals is equivalent to a vanishing cross-correlation product or cross-correlation function (CCF). For the CCF, meaningful integration bounds must be considered, for example, integration over one symbol period. For optical WDM, the requirement (1.1) is easily fulfilled. Given that the different wavelength channels, including the Fourier transform-induced broadening due to the modulation, are properly spaced in the wavelength domain, any two different passbands of the WDM multiplexing (MUX) and demultiplexing (DMX) filters are orthogonal with respect to each other. In reality, Eq. (1.1) may not be achieved exactly, but only approximately due to linear or nonlinear cross talk.

WDM is the generalization of frequency-domain multiplexing that is long known from radio and coaxial transmissions. With a WDM channel, it can be combined with any other of the known electrical multiplexing or multiple-access schemes. These include electrical frequency-domain multiplexing, which is then referred to as subcarrier multiplexing (SCM), time-domain multiplexing (TDM), and code-domain multiplexing. One scheme of particular interest for both the multiplexing and multiple access is orthogonal frequency-domain multiplexing (OFDM), which can be applied within a wavelength channel or covering the optical frequencies of several wavelength channels. The respective multiple access schemes are time-domain multiple access (TDMA), subcarrier multiple access (SCMA), frequency-domain multiple access (FDMA), and code-domain multiple access (CDMA).

1.2 HISTORY OF WDM

The development toward commercial WDM transport systems as the common basis of all metropolitan area, regional, national, and international telecommunications networks was enabled by a number of relevant milestones:

- 1960: first laser developed [1]
- 1966: first description of dielectric waveguides as a potential means for data transmission by Kao and Hockham [2]
- 1970: first low-loss optical fiber produced (~20 dB/km) [3,4]
- 1976: first InGaAsP diode laser for 1300 nm window produced [5]
- 1978: first low-loss single-mode fiber produced (~0.2 dB/km) [6]
- 1978: first experimental WDM systems developed [7]
- 1987: first Erbium-doped fiber amplifier (EDFA) developed [8,9]
- 1995: first commercial WDM systems available

These milestones were accompanied by the development of ever-improved components (e.g., diode lasers for the 1550 nm window) and various types of single-mode fibers.

High-speed single-mode fiber transmission started in 1981 with single-channel transmission at ~1300 nm. Reasons were the availability of suitable semiconductor diode lasers and the fact that the first single-mode fibers [which are meanwhile referred to as standard single-mode fibers (SSMF)] had their region of lowest chromatic dispersion (CD) around 1300 nm. CD was the strongest deteriorating effect for early fiber transmission, limiting maximum reach. In addition, the region around 1300 nm had lowest fiber attenuation for wavelengths lower than the water-peak absorption region. The next step—for single-channel transmission—was to align the regions of lowest CD and lowest fiber attenuation in order to further maximize reach, in particular for the upcoming 10 Gb/s transmission. Since fiber attenuation is basically a material characteristic that cannot be influenced significantly for silica fibers, the region of lowest CD had to be shifted to ~1550 nm in order to align both parameters. CD can be shifted since it depends on both the material and waveguide (geometry) characteristics. Hence, it can be shifted by designing a suitable radial refractive index profile. This has been done around 1990, and the result is the so-called dispersion-shifted fiber (DSF)—sometimes also referred to as dispersion-shifted single-mode (DSSM) fiber. DSF was heavily deployed in Japan and certain other regions (e.g., parts of the United States and Spain).

The deployment of DSF badly interfered with the usage of first WDM systems. The problem was caused by transmitting several WDM channels around 1550 nm, at close-to-zero CD. The EDFA, which had meanwhile been invented and which revolutionized long-reach fiber transmission, enabled long transparent link lengths exceeding 600 km. With increasing transparent link lengths and increasing total and per-channel fiber launch power, a fiber characteristic—nonlinearity—got relevant that had not been considered seriously before. Though basic work on fiber nonlinearity had been published in the 1970s (see Section 2.2), one of the nonlinear effects, four-wave mixing (FWM), now started to seriously limit WDM transmission on real-world fibers. FWM is the parametric mixing effect that occurs due to the fundamental fiber's cubic Kerr nonlinearity. As with all parametric mixing, it relies on phase matching between the mixing waves that can be achieved in real fiber in the *absence* of CD. This was just the design goal for single-channel transmission DSFs. Once it efficiently occurs, FWM cannot be counteracted anymore; it thus fundamentally limits reach.

The problem with WDM transmission on fibers with close-to-zero CD then led to the development of a family of modified single-mode fibers. These fiber designs, known as nonzero dispersion-shifted fibers (NZ-DSF) or dispersion-flattened single-mode (DFSM) fibers, followed the idea to provide nonzero CD that is yet smaller than that in SSMF in order to reduce both the linear and nonlinear distortions. The second-generation WDM systems could achieve approximately the same maximum reach (which was still limited in the 600 km range) on SSMF and NZ-DSF. With transparent reach extended into the ultralong-haul domain and the techniques for optical CD compensation having been developed during the 1990s, it turned out that nonlinear distortions were still the dominating reach limitation. This led to the development of several NZ-DSF with increased (and also flattened) CD. Finally,

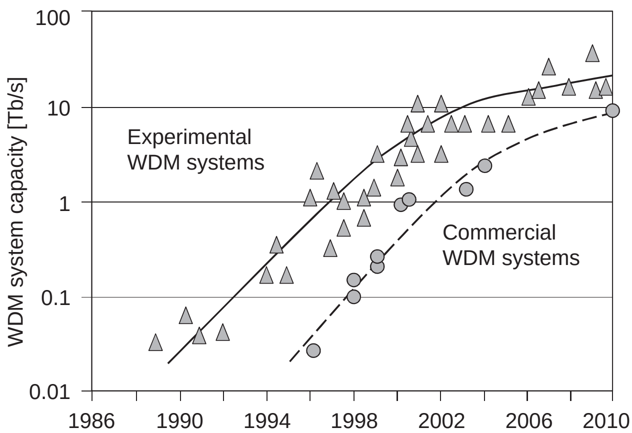

FIGURE 1.1 Development of WDM systems transport capacity over time.

with the product of transparent reach and total capacity (in terms of number of WDM channels and per-channel bit rate) further increasing, it turned out that in the presence of nonlinearity, SSMF with their high CD are the optimum choice of silica fibers. Further improvements of the bandwidth-reach product will likely require disruptive new fiber types.

Driven by improvements of components and modulation and equalization techniques, the total transport capacity of WDM systems has largely increased since the first experiments with WDM. This is shown in Fig. 1.1 for both the experimental and commercial WDM systems.

Two aspects can be derived from Fig. 1.1. First, commercial WDM systems are following "hero" experiments somewhat more timely now and both are approaching an area of slowed down capacity improvement. Over the next few years, WDM on SSMF will finally reach what is now known as the nonlinear Shannon limit [10]. Further progress beyond this limit will require new fiber types.

REFERENCES

1. T.H. Maiman, Stimulated optical radiation in ruby, Nature, Vol. 187, No. 4736, 1960, pp. 493–494.
2. K.C. Kao and G.A. Hockham, Dielectric-fibre surface waveguide for optical frequencies, Proc. IEEE, Vol. 113, No. 7, 1966, pp. 1151ff.
3. D.B. Keck et al., On the ultimate lower limit of attenuation in glass optical waveguides, Appl. Phys. Lett., Vol. 22, No. 7, April 1973, pp. 307ff.
4. P.C. Schultz Making the first low loss optical fibers for communications, ECOC2010 Torino, September 2010.
5. J. Hsieh et al., Room-temperature cw operation of GaInAsP/InP double-heterostructure diode lasers emitting at 1.1 μm, Appl. Phys. Lett., Vol. 28, No. 12, 1976, pp. 709–711.

6. H. Murata and N. Inagaki, Low-loss single-mode fiber development and splicing research in Japan, IEEE J. Quantum Electron. Vol. 17, No. 6, June 1981, pp. 835–849.
7. W.J. Tomlinson and C. Lin, Optical wavelength-division multiplexer for the 1–1.4-micron spectral region, Electron. Lett., Vol. 14, May 1978, pp. 345–347.
8. R.J. Mears et al., Low-threshold tunable CW and Q-switched fiber laser operating at 1.55 μm, Electron. Lett., 22, 1986, pp. 159–160.
9. R.J. Mears et al., Low-noise erbium-doped fiber amplifier at 1.54 μm, Electron. Lett., Vol. 23, 1987, pp. 1026–1028.
10. R.-J. Essiambre et al., Capacity limits of optical fiber networks, IEEE J. Lightwave Technol., Vol. 28, No. 4, 2010, pp. 662–701.

2

OPTICAL FIBER EFFECTS

2.1 LINEAR EFFECTS

Wavelength division multiplexing (WDM) transmission heavily depends on the fiber type that is used, and the related transmission effects and characteristics. Single-mode fibers are transmission systems that show frequency dependence (i.e., the pulse response is not the Dirac delta function), time variance, and weak nonlinear behavior. The resulting transmission impairments are as follows:

- *Linear Effects*
  - Attenuation (intrinsic loss, bending loss)
  - Polarization-dependent loss (PDL)
  - Chromatic dispersion (CD) due to material waveguide, and profile dispersion. These dispersion mechanisms lead to
    - Group-velocity dispersion (GVD)
    - Dispersion slope or higher order CD
  - Polarization-mode dispersion (PMD) including higher order PMD
- *Nonlinear Effects*
  - Self-phase modulation (SPM)
  - Cross-phase modulation (XPM, IXPM)
  - Four-wave mixing (FWM, IFWM)

Wavelength Division Multiplexing: A Practical Engineering Guide, First Edition.
Klaus Grobe and Michael Eiselt.

- Modulation instability
- Nonlinear phase noise (NLPN)
- Cross-polarization modulation (XPolM)
- Stimulated Raman scattering (SRS)
- Stimulated Brillouin scattering (SBS)

Detailed discussions of these effects can be found in the literature [1,2]. For WDM long-haul transmission, all these effects and their interactions have to be considered.

2.1.1 Attenuation

Attenuation in silica optical single-mode fibers is caused by different effects:

- Intrinsic loss of silica glass
  - Rayleigh scattering
  - Infrared absorption
- Extrinsic loss due to impurity of the silica glass
- Bending loss
  - Macrobending loss
  - Microbending loss
- Polarization-dependent loss

Attenuation in an optical transmission fiber can be described with a linear, frequency-dependent and (with the exception of PDL) time-invariant transfer function.

2.1.1.1 Intrinsic Loss Intrinsic loss in silica fibers leads, in lateral or z-direction, to an exponential power loss. This power loss can be described by a transfer function $H_a\,(z,\,\omega)$:

$$H_{\mathrm{a}}(z,\omega) = \mathrm{e}^{-\alpha_{\mathrm{p}}(\omega)z}. \tag{2.1}$$

Here, ω is the angular frequency, and $\alpha_p(\omega)$ is the attenuation constant with dimension (1/m).

Rayleigh scattering is caused by density fluctuations that occur in microscopic regions with dimensions smaller than the optical wavelengths. They are unavoidably caused during manufacturing of the glass rod when a certain stochastic density distribution of the glass is fixed. These density fluctuations cause scattering of electromagnetic waves. Light being scattered out of the z-direction has a randomly distributed phase. Due to interference, the resulting light propagating perpendicular to the z-direction cancels almost exactly. Only a small fraction interferes constructively and is scattered out of the original (z) direction. This is the Rayleigh scattering loss. The light scattered in forward direction adds coherently without any further attenuation. This mechanism is also called *elastic scattering*.

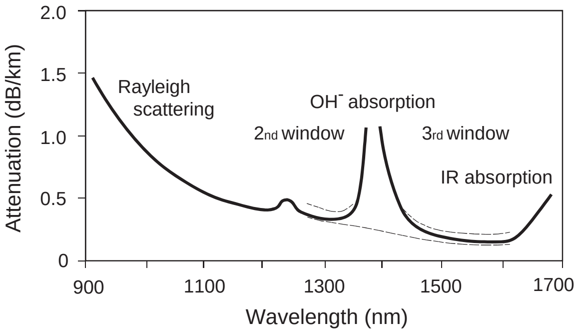

FIGURE 2.1 Spectral loss in single-mode fibers.

Rayleigh scattering is proportional to λ^{-4}, where λ is the optical wavelength. At 1550 nm, the attenuation caused by Rayleigh scattering is in the range of 0.12–0.16 dB/km. In this wavelength region, Rayleigh scattering is the dominant source of intrinsic loss [1].

Infrared absorption is caused by absorption through vibrational resonances in the infrared regime with wavelengths larger than 7 μm. In silica glass, there are also electronic resonances in the UV regime below 400 nm that do not contribute to loss significantly. Due to the amorphous structure of glass, the vibrational resonances form absorption bands that are spaced as far as into the regime of visible optical wavelengths. In the range of 800–1550 nm, the loss caused by infrared absorption is below 0.1 dB/km [1].

The spectral loss caused by intrinsic effects and impurity is shown in Fig. 2.1. The attenuation peak in the wavelength region around 1400 nm is caused by OH^- ions. In old fibers (vintages up into the 1980s), this peak was very pronounced, while in new fibers, it has been eliminated by means of better production methods (better clean-room environment). The dashed lines in Fig. 2.1 indicate the minimum and maximum loss tolerance as specified in the ITU-T Recommendation G.695 for standard single-mode fibers.

2.1.1.2 Fiber Bending Loss Fiber-optic waveguides not only exhibit loss due to intrinsic effects and impurity but also exhibit loss caused by perturbations of the ideal waveguide geometry. Such perturbations can result from bending the fiber, where bending radii with $R \gg \lambda$ and $R \approx \lambda$ with λ the optical wavelength have to be considered separately. Loss caused by bending radii $R \gg \lambda$ is called macrobending loss, for $R \approx \lambda$, microbending loss occurs. Both kinds of bending loss can result from incorrect handling of fibers like bad cabling with tight bends.

Macrobending loss occurs because part of the electromagnetic field that is normally guided in and near the core of the fiber is radiated out of the fiber in a bend. This happens because *phase planes* propagate in the fiber as long as the medium is homogenous and isotropic. The phase planes are orthogonal to the wave vector k. In a fiber bend, propagation is still based on phase planes that are orthogonal

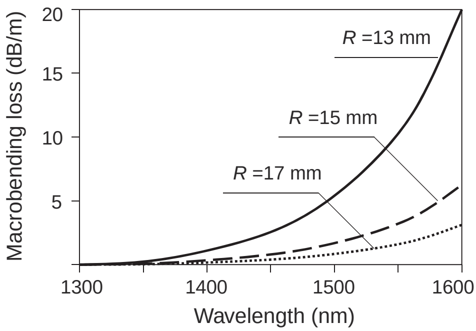

FIGURE 2.2 Macrobending loss in standard single-mode fibers (G.652A).

to the direction of propagation and hence follow the geometry of the bend. In order to maintain phase planes orthogonal to k, the planes now have to propagate at constant *angular* velocity. Those parts of the plane that are *outside* the middle axis of the fiber have to propagate at higher velocity than the ones *inside*. Along the middle axis of the fiber, the plane propagates with a velocity of $c_{\mathrm{Co}} = c_0/n_{\mathrm{Co}} = R \cdot \mathrm{d}\phi/\mathrm{d}t$, with c_{Co} the velocity of light in the core of the fiber, c_0 the velocity of light in vacuum, n_{Co} the refractive index of the core, R the bending radius, and $\mathrm{d}\phi/\mathrm{d}t$ the angular velocity. At a critical radius $R_{\mathrm{C}} = n_{\mathrm{Co}}/n_{\mathrm{Cl}} \cdot R$, the maximum allowed velocity of $c_{\mathrm{Cl}} = c_0/n_{\mathrm{Cl}}$ is exceeded in the optical cladding of the fiber. Here, n_{Cl} is the refractive index of the optical cladding. Beyond R_{C}, no phase planes orthogonal to k are possible anymore, hence the respective parts of the field must be radiated out of the fiber and contribute to bending-induced loss.

Macrobending loss can be calculated using mode coupling or antenna theory [3–6]. It increases exponentially with increasing wavelength and decreasing bending radii. Typical macrobending loss for a single-mode fiber (according to ITU-T Recommendation G.652A) is shown in Fig. 2.2.

For wavelengths <1300 nm and bending radii >20 mm, macrobending loss can be neglected in most cases. The DWDM wavelength region around 1550 nm can already be affected significantly, for example, by sharp bends of patch cables. The region >1600 nm is very sensitive to macrobending. For these reasons, low-bending loss fibers have been developed more recently (they are specified in the ITU-T Recommendation G.657).

Microbending loss is caused when the fiber, including its buffer/coating, is subject to radial pressure. This can happen when a fiber is brought into a cable that is then put under radial mechanical pressure [7,8]. The pressure forces deformations of the boundary between core and cladding of the fiber that have similar dimension as the wavelength. This causes interference between light that is scattered out of its original direction and consequently loss. Microbending loss can be described as a stochastic process. If fibers are cabled correctly, it can usually be neglected. The effect, however, can be useful in certain fiber sensors (e.g., for detecting mechanical pressure).

2.1.1.3 Polarization-Dependent Loss WDM transmission systems with optical amplifiers and other passive components in the optical path are vulnerable to performance degradation due to PDL. A similar effect in active components is polarization-dependent gain (PDG) [9]. PDL can be caused by optical components such as directional couplers and isolators, while PDG is caused by polarization hole burning in optical amplifiers. Due to PDL and PDG, a polarized signal may be attenuated or amplified differently than unpolarized noise, and the signal-to-noise ratio (SNR) is modified accordingly. These SNR modifications lead to performance degradation. Since the state of polarization (SOP) of the transmitted light is randomly changed in time, PDL and PDG may cause the system performance to vary in a random manner as a function of time.

Distributed PDL and PDG in a high-PMD link also changes the characteristics of the PMD. The principal states of polarization (PSP) will not be orthogonal anymore. PMD-induced pulse spreading can become larger. Also, the distribution of the differential group delay (DGD) may not be Maxwellian anymore. This in turn can lead to severe under- or overestimation of DGD.

With a growing number of PDL elements, the probability density function (PDF) of PDL (in dB) approaches a Maxwellian distribution. The mean PDL then grows with increasing number of elements N like [10]

$$\langle \mathrm{PDL} \rangle = \mathrm{PDL}_i \cdot \sqrt{\frac{8}{3\pi} \cdot N}. \tag{2.2}$$

Effects of PDL and PDG are difficult to be quantized due to their interaction with PMD. In long transmission links with a large number of PDL-prone components, a PDL-related penalty must be taken into consideration. An example for the PDL penalty for an ultralong-haul link is given in Fig. 2.3 [9].

For this example, a transmission link of almost 9000 km total length with 270 EDFAs has been considered.

2.1.2 Chromatic Dispersion

CD causes signal distortions through the dependence of the velocity of propagation (the group velocity) on the frequency of the respective spectral components. Since every information transmission requires at least Fourier-limited spectral broadening

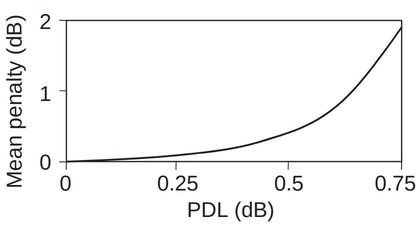

FIGURE 2.3 PDL-induced SNR penalty in long-haul transmission.

due to the respective modulation of the carrier wave, every information transmission in optical fibers is subject to CD.

CD can be described by a linear, (mostly) time-invariant system with memory. Since different spectral components of a signal, that is, a pulse carrying digital information, propagate at different velocities, the resulting effect is a temporal spread of the signal. In digital transmission, this spread leads to intersymbol interference (ISI). The effect is also known as intramode dispersion [11]. It can further be split into

- material dispersion,
- waveguide dispersion,
- profile dispersion.

Material dispersion results from interactions of a propagating electromagnetic wave with the bonding electrons of the surrounding matter. It depends on the frequency ω of the wave and can be described as the frequency dependence of the refractive index $n(\omega)$. $n(\omega)$ can be derived from the Sellmeier series that considers the relevant resonances that are responsible for the wave-matter interactions [2]:

$$n^2 = 1 + \sum_{i=1}^{3} B_i \cdot \frac{\omega_i^2}{\omega_i^2 - \omega^2}. \tag{2.3}$$

The resonance frequencies ω_i are weighted with weights B_i. The relevant values for silica fibers are summarized in Table 2.1. Here, $\lambda_i = 2\pi \cdot c/\omega_i$ and c are the respective wavelength and the speed of light in silica glass, respectively.

Material dispersion can also be assigned a material dispersion parameter D_{mat}:

$$D_{\mathrm{mat}} = -\frac{\lambda}{c}\frac{\mathrm{d}^2 n}{\mathrm{d}\lambda^2}. \tag{2.4}$$

Here, n is the refractive index of the bulk material. The negative sign indicates that low-wavelength components arrive before higher wavelength components

Waveguide dispersion appears because the light waves are guided in a waveguide with certain geometrical shape and dimensions. The effect is caused by the dependence of the eigenvalues of the wave propagation equation on the relation between waveguide cross-sectional dimensions and wavelengths of the propagating signal. Compared to material dispersion, waveguide dispersion is a weak effect but as compared to bulk silica, it shifts the wavelength region of lowest CD toward longer

TABLE 2.1 Sellmeier Coefficients

$B_1 = 0.6961663$	$\lambda_1 = 0.0684043\ \mu\mathrm{m}$
$B_2 = 0.4079426$	$\lambda_2 = 0.1162414\ \mu\mathrm{m}$
$B_3 = 0.8974794$	$\lambda_3 = 9.8961610\ \mu\mathrm{m}$

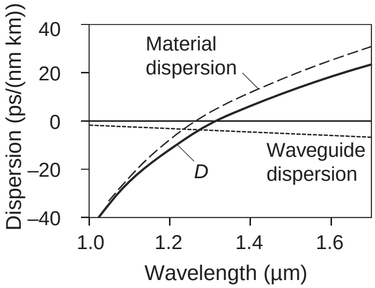

FIGURE 2.4 Waveguide and material dispersion.

wavelengths. Lowest-dispersion wavelengths are $\lambda_0 \approx 1270\,\text{nm}$ for bulk silica and $\lambda_0 \approx 1310\,\text{nm}$ for standard single-mode fibers [2]. This effect is shown in Fig. 2.4.

Profile dispersion describes the dependence of the radial refractive index profile $n(r)$ on the wavelength. $n(r)$ is determined by the refractive indices of the core and its cladding(s), and the core diameter. It depends on the wavelength because core and cladding(s) consist of differently doped glass with different dependencies of the refractive indices on wavelength [12]. It is the weakest of the chromatic dispersion effects.

In the absence of nonlinearity and birefringence, propagation of a light wave with envelope E is given by

$$E(z,t) = E_0\, \mathrm{e}^{j(\omega t - kz)} = E_0\, \mathrm{e}^{-\alpha z}\, \mathrm{e}^{j(\omega t - \beta z)}. \tag{2.5}$$

The effect of chromatic dispersion is described by the complex wave number $k(\omega)$ that splits into attenuation constant $\alpha(\omega)$ and phase constant $\beta(\omega)$:

$$k(\omega) = \beta(\omega) - j\alpha(\omega). \tag{2.6}$$

For practical calculations, $\alpha(\omega)$ is often considered a constant. Alternatively, it can be calculated via the Sellmeier series [1], or via Hilbert transform of $\beta(\omega)$. The phase constant is usually developed into a Taylor series around a mean carrier frequency ω_0, for example, 1550 nm:

$$\beta(\omega) = \beta_0 + \beta_1(\Delta\omega) + \frac{\beta_2}{2!}(\Delta\omega)^2 + \frac{\beta_3}{3!}(\Delta\omega)^3 + \cdots, \tag{2.7}$$

$\Delta\omega$ is given by $\omega - \omega_0$. The Taylor coefficients β_i can be derived as

$$\beta_i = \left.\frac{\mathrm{d}^i \beta(\omega)}{\mathrm{d}\omega^i}\right|_{\omega_0}. \tag{2.8}$$

From the Taylor series, some velocities and dispersion parameters can be derived.

The *phase velocity* is given by $v_\mathrm{P} = \omega_0/\beta_0 = c_0/n$. It is irrelevant for information transmission since it relates to an unmodulated (monochromatic) wave. Under certain conditions, the phase velocity is also allowed to exceed the vacuum speed of light c_0 (which is forbidden for any information–transmission velocity).

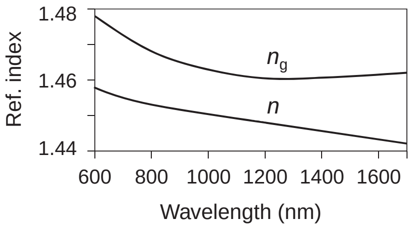

FIGURE 2.5 Fiber group index.

The coefficient β_1 leads to the *group velocity* v_g and the group index n_g. The group index is inverse proportional to v_g that is the relevant parameter for the velocity of the information transfer in media with *normal* dispersion (i.e., $dn/d\omega > 0$, and $0 < v_g < c_0$). However, under certain conditions of *anomalous* dispersion, the group velocity may be greater than the speed of light or even negative and then does not represent the velocity of energy flow or information transmission. In this case, information–transmission velocity is given by the so-called group-front velocity that is smaller than c_0 [13,14].

The group velocity is given through the Taylor coefficient β_1:

$$v_g = 1/\beta_1 = c_0/n_g. \tag{2.9}$$

The group velocity is also given through the fiber group index that is shown in Fig. 2.5.

The next coefficient, β_2, describes chromatic group-velocity dispersion. For the description of transmission systems with up to ~10 Gb/s, this coefficient is sufficient. If transmission at very high bandwidths—ultrahigh-speed TDM and/or WDM—must be calculated, the next coefficient, β_3, has to be considered as well. β_3 describes the dispersion slope of the respective fibers, or higher order dispersion.

β_2 is often described via the dispersion parameter D [1,2]:

$$D = -\omega^2\beta_2/2\pi c_0. \tag{2.10}$$

This parameter has dimension [ps/(nm km)]. It describes the temporal spread (in ps) of signal pulses with a certain optical bandwidth (in nm) over a certain transmission distance (in km).

Figure 2.6 lists D parameters for relevant single-mode fiber types (according to ITU-T Recommendations G.652, G.653, G.655), as well as brands of fibers (G.655 TW-RS®, G.655 LEAF®, SMF-LS™ NZ-DSF).

For almost all single-mode fibers, the D parameter crosses zero somewhere between 1300 and 1550 nm, that is, in the wavelength region of interest. Around that particular wavelength, fibers have low chromatic dispersion. The zero-crossing also splits the spectrum into two distinct domains: smaller wavelengths exhibit normal dispersion (negative D, positive β_2), and wavelengths above the zero-crossing have

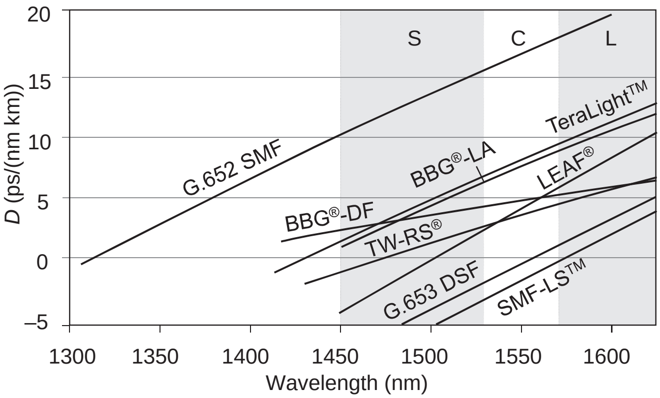

FIGURE 2.6 *D* parameters of various single-mode fibers.

anomalous dispersion (positive D). For normal dispersion, spectral components with *higher* frequencies (blue-shifted) are propagating *slower* than those at lower frequencies (red-shifted). For anomalous dispersion, blue-shifted components are traveling faster than red-shifted components.

The D parameter can be used to define a linear transfer function that considers CD:

$$H_{\mathrm{CD}}(z, j\omega) = \exp\left[j\left(\beta_0 + \beta_1(\omega - \omega_0) - \frac{1}{2}\frac{\lambda_0^2}{2\pi c_0}D(\omega - \omega_0)^2\right)z\right]. \tag{2.11}$$

Propagation of a slowly varying pulse envelope $A(\omega, l)$, is then given by

$$A(\omega, L) = \exp\left(\frac{j}{2}\cdot\beta_2\omega^2 L\right)A(\omega, 0). \tag{2.12}$$

The transfer function $H_{\mathrm{CD}}(z, j\omega)$, together with a suitable consideration of the attenuation (which may be a constant attenuation coefficient), can be used for calculations or simulations of a linear fiber model that neglects the nonlinear effects.

The D parameter can be used for a simplified approximation of the bandwidth that can be utilized for a transmission fiber link with given length. The 3 dB bandwidth $f_{3\,\mathrm{dB}}(z)$ is

$$f_{3\,\mathrm{dB}}(z) \approx \frac{3}{4|D|z\,\Delta\lambda}. \tag{2.13}$$

Here, $\Delta\lambda$ is the optical bandwidth. Equation (2.13) allows an approximation of the maximum transparent field length (i.e., the maximum distance between two terminations or 3R-regenerators, and without CD compensation) for transmission at a given bit rate and using a given modulation scheme, for example, NRZ-OOK with direct detection. The corresponding GVD-limited maximum link length depending on the bit rate is shown for NRZ-OOK in Fig. 2.7.

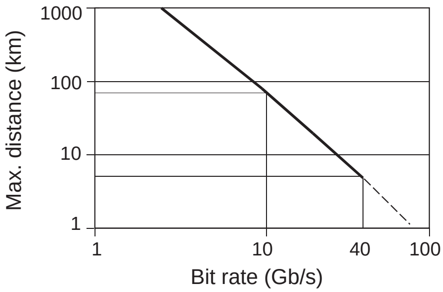

FIGURE 2.7 Maximum distance limitation caused by uncompensated GVD on G.652 fibers.

It is obvious from Fig. 2.7 that simple on–off keying (OOK) is not sufficient for very high bit rates in excess of 10 Gb/s. However, OOK can still be used for serial short-reach interfaces at 40 Gb/s that aim at a maximum reach of 2 km, and similar applications.

2.1.3 Polarization-Mode Dispersion

2.1.3.1 PMD and DGD Polarization-mode dispersion is caused by birefringence of the transmission fibers, that is, the effective refractive index is different between two orthogonal polarizations. This birefringence, in turn, is caused by fiber geometry imperfections or by lateral stress on the fiber, leading to two orthogonally polarized (OP) modes propagating at slightly different velocities [15]. The geometry imperfections occur during fiber manufacturing and cabling of the fibers (i.e., bringing the fibers into a cable), and also during deployment of the fiber-optic cables. They cannot be fully suppressed during manufacturing and deployment.

While in a perfectly circular fiber no particular pair of orthogonal polarization modes is distinguished, birefringence leads to two particular modes standing out. These modes are referred to as the principal states of polarization. They usually depend on the frequency (or wavelength) of the optical signal. The PSPs are defined at the input to the fiber as those states of polarization, for which, when slightly varying the signal frequency, the output polarization remains constant. Even if a single polarization mode is excited at the transmitter—like in a typical laser—this mode not necessarily coincides with a fiber PSP such that both PSPs are excited within the fiber.

Over a given transmission length, the time delay between both PSPs is given by the DGD. The PSPs as well as the DGD are wavelength dependent and also vary over time with changing environmental impact. As the statistics over time and wavelength theoretically follow the same Maxwellian distribution, the average value of the DGD over time and over wavelength are equal. This number is commonly referred to as the PMD of a fiber span. The effect of PMD is visualized in Fig. 2.8.

Polarization and its related effects are represented by the Stokes parameters and can be visualized on the Poincaré sphere. The relationship of the Stokes parameters (as components of the Stokes vector $\vec{S}$) to intensity and polarization ellipse